

LETTERS

Tailoring calcite: Nanoscale AFM of coccolith biocrystals

K. HENRIKSEN,¹ S.L.S. STIPP,^{1,*} J.R. YOUNG,² AND P.R. BOWN³

¹Geological Institute, University of Copenhagen, Øster Voldgade 10, DK-1350 Copenhagen K, Denmark

²Natural History Museum, Cromwell Road, London SW7 5BD, U.K.

³Department of Geology, University College London, Gower Street, London WC1E 6BT, U.K.

ABSTRACT

Biom mineralization produces crystals of elaborate shapes, never seen in inorganic mineralogy, with tightly regulated compositions and axis orientations. The calcite coccoliths produced by unicellular marine algae provide an example of such control at very tiny scales. Atomic force microscopy (AFM) of two species provided nanoscale images allowing us to define crystallographic orientation in the crystal elements and to establish the relationship between crystallographic orientation and coccolith morphology. Both species adopt the inorganically stable calcite rhomb, but differences in crystal orientation enable them to construct distinct architectures with properties tailored to suit the requirements of their ecological niche.

INTRODUCTION

Organisms tailor minerals into highly complex functional structures, exerting control on composition, crystallographic orientation, and morphology to the extent that biocrystals often bear virtually no resemblance to their inorganic counterparts. The aragonite in coral or the fantastically elaborate single calcite crystals that make up sea urchin shells are examples of biominerals that challenge us to demonstrate the relationship between morphology and crystal lattice. Understanding the relationship between crystallographic orientation and structure is a requirement for determining how the organisms achieve their intriguing control on mineral expression.

Coccoliths (Fig. 1) are calcite shields produced by unicellular marine algae (haptophytes). They demonstrate that biological crystal regulation is possible at very tiny scales. Most coccoliths are double discs consisting of several radially arranged elements of complex morphology, but the total size of the structure is typically less than 12 micrometers. Several coccoliths interlock to form a hollow sphere, called a coccosphere, around the alga. Microscopy, using polarized light (PLM), scanning electron (SEM), and transmission electron (TEM) beams, has shown that each element is a separate crystal and that coccoliths originate in intracellular compartments from a “protococcolith ring” of crystal nuclei with alternating crystallographic orientation, probably controlled by an organic template. For many species, half of the nuclei are “V units” where the c-axis lies roughly vertical to the shield, and the other half are “R units” where the c-axis is sub-radial (Young et al. 1999, 1992). Unfortunately, however, PLM and SEM reveal only the direction of the c-axis vector, and that only approximately. They cannot disclose details of crystallographic orientation.

Atomic force microscopy (AFM) can provide such information, through its ability to image the atomic pattern on the

surface. AFM studies of the cleavage surface of inorganically precipitated calcite have revealed its characteristic appearance at the micrometer scale and described the details of the atomic pattern (Stipp et al. 1994; Stipp 1999). AFM records force interaction between the tip and the outermost atoms of the surface. In the case of calcite, the tip images the topmost O atoms that octahedrally coordinate Ca. These O positions would be filled by O from CO₃ groups in the bulk structure, but after cleavage or during growth, the dangling bonds, i.e. the empty positions, over the Ca-octahedra are filled by the OH of hydrolyzed water (Stipp and Hochella 1991; Stipp 1999). The bonds between the topmost O atoms and the dangling 1/3+ charge over the surface Ca atoms is strong enough that the scanning AFM tip records an elevation maximum in those positions, but the bonds are weak enough to allow replacement by CO₃ groups when the crystal grows. The length of the bond and its position out from the surface allow the topmost O to be influenced as it is scanned by the AFM tip. One can observe the interaction as a relative displacement of maxima on the AFM image, with the extent of displacement depending on the direction of scanning relative to the direction of the carbonate rows (Stipp 1999). The result is a pairing of rows within the calcite unit cell that is characteristic and that can be used to define the orientation of the crystal.

Atomic force microscopy of coccoliths at a variety of scales has revealed the detailed morphology of the mineral surface and associated organic coating, and we investigated the influence of the organic material on behavior during dissolution. These aspects are presented in Henriksen et al. (2004).

The purpose of this study was (1) to collect AFM images of coccoliths at a variety of scales ranging from several micrometers for whole shields to atomic scale; (2) to define crystallographic orientation of the coccolith elements; and (3) to establish the relationship between crystal orientation and coccolith morphology and function. Although several nanoscale studies of inorganic, single-crystal calcite surfaces have been

* E-mail: stipp@geol.ku.dk

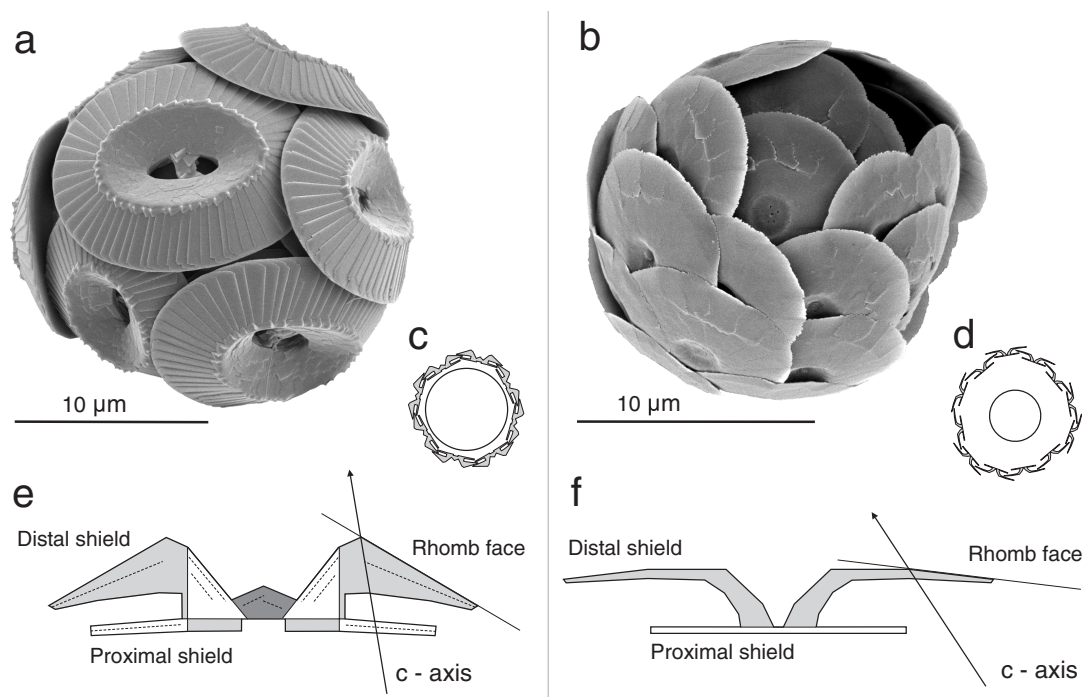


FIGURE 1. Scanning electron micrographs of coccospheres of (a) *Coccolithus pelagicus* and (b) *Oolithotus fragilis*. (c) Schematic cross-section through coccosphere and cell of *C. pelagicus*. The coccoliths are rather bulky and close to the cell wall, resulting in a relatively high total density and (d) *O. fragilis*. The coccoliths are thin and the coccosphere incorporates a large envelope of seawater; surface area is increased, density, decreased. (e) Schematic profile showing coccolith structure with R-units in white, V-units in light grey and central structures in dark grey. Dashed lines indicate presence of internal grain boundaries, rhomb faces and c-axis orientation shown for *C. pelagicus*. Note that in the third dimension, the rhomb face is tilted so that the c-axis is close to vertical. (f) *O. fragilis*. The c-axes of 'V-units' are positioned about 30° away from vertical.

published, to the best of our knowledge, such high-resolution imaging of natural, biogenic, and uncleaved calcite has not been achieved previously.

EXPERIMENTAL DETAILS

We used a Digital Instruments Nanoscope Multimode IIIa AFM running in contact mode, with a scanner with maximum x- and y-offsets of 13 μm . Tips were commercially available, sharpened Si_3N_4 pyramids integrated on a gold-coated cantilever with a spring constant of about 0.6 nN. Samples were imaged in a glass fluid cell with the O-ring removed for easier selection of scan-area and to minimize image distortion from O-ring creep. To minimize random oscillation in the images arising from building vibration and sound, the AFM was hung on a vibration-dampening platform suspended from the ceiling on rubber-cords and covered by hoods of aluminum and foam. Distortion in AFM, arising from non-linearity in the scanning process, influences both angular relationships and distances, complicating image interpretation. However, images can be corrected for distortion using the method described by Henriksen and Stipp (2002), so we applied this procedure to our atomic scale scans. Distortion parameters are specific to an image; they have been included in the figure captions. Because drift, the component of distortion that influences angular relationships, decreases with instrument operation time (Henriksen and Stipp 2002), we used only images taken after 70 minutes to approximate angles in the micrometer-scale images.

The physics of the AFM imaging process has been discussed extensively in the literature (Binnig 1992; Ohnesorge and Binnig 1993; Sokolov et al. 1999), and there is general agreement that AFM images are often Moiré or interference patterns produced by the overlapping of signals from multiple tips. Double or multiple tips can either obscure atomic row-pairing or make it appear that the lower row is really the higher of the

pair. True row-pairing images have rows where corrugations are clearly defined with space between; there is no change along the row from higher to lower or vice versa; and the pattern is consistent over many nanometers in both x- and y-directions. The corrugations need not all be round; in fact, some of the clearest images have rows of rounded spots alternating with rows of elongated spots (Fig. 2e and Stipp et al. 1994). With true row-pairing images, the higher row of the pair always faces the acute edges of the rhomb.

We investigated the distal or outer shields of coccoliths from two species, *Coccolithus pelagicus* and *Oolithotus fragilis* (Fig. 1), which thrive in very different habitats. The samples were obtained from mono-specific algal cultures grown at the Natural History Museum, London and the University of Caen, France. Culture material was spun repeatedly in a centrifuge and resuspended in a buffer solution of 0.05 m NH_4HCO_3 , to rinse the salt from the culture medium while preventing dissolution of the coccoliths. The same buffer was used during imaging in the fluid cell.

RESULTS AND INTERPRETATION

Figure 2a shows a complete distal (outer) shield of *Coccolithus pelagicus*. This species produces thick coccoliths composed of 30 to 60 imbricated elements. The triangular and linear features outside the circumference of the shield are AFM imaging artifacts that result when the pyramidal tip moves down over the sharp shield edge, which is very tall relative to the

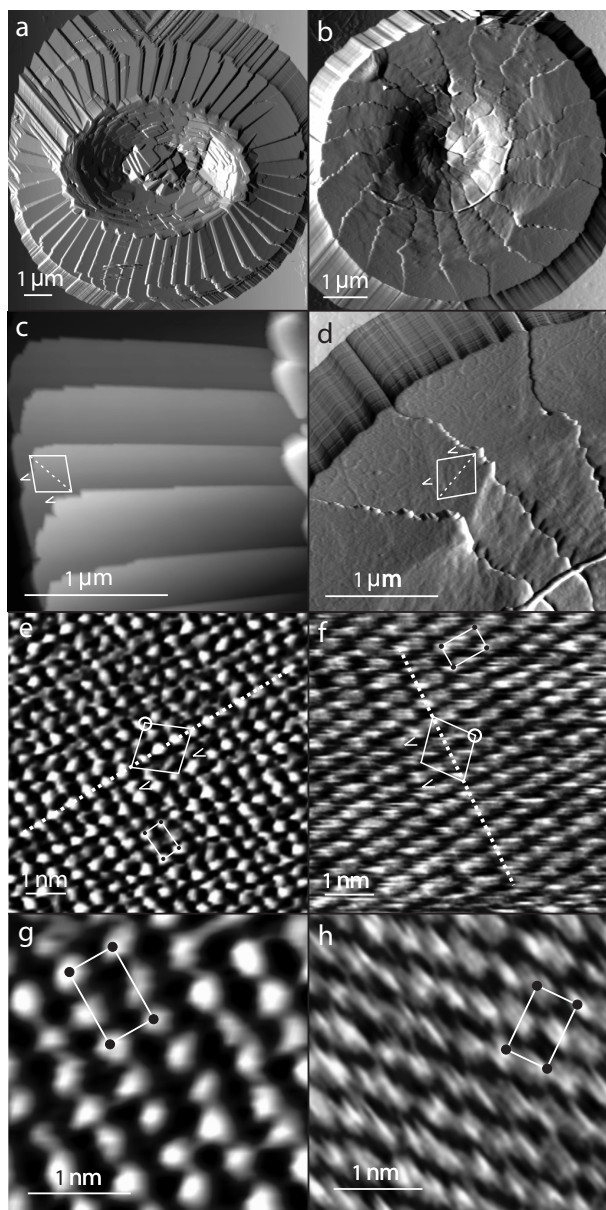


FIGURE 2. Atomic force microscopy images. Coccoliths of (a) *C. pelagicus* and (b) *O. fragilis*. (c) Distal shield elements of *C. pelagicus*. Outlined are directions of the calcite rhomb (white) and atomic rows (dashed); < indicates rhombic crystal faces that slope away at an acute angle (defined using the information given by atomic scale images). (d) *O. fragilis*. (e) Atomic pattern showing row-pairing on distal shield elements of *C. pelagicus*; a-axis shown by dotted line, surface unit cell with dimensions $4.99 \times 8.10 \text{ \AA}$ outlined and orientation of cleavage rhomb shown; < marks faces sloping away at acute angles and the open circle marks the intersection of the obtuse sides, where the c-axis emerges. All images are unfiltered, but the high-resolution images have been corrected for distortion by the method outlined in Henriksen and Stipp (2002), for this image with factors for drift of 0.1 nm/s and scaling of 1.03. (f) *O. fragilis* (corrected for drift: 0.3 nm/s, scaling: 1.11). The atomic spacing and structure on both are characteristic of the $\{10\bar{1}4\}$ rhombic crystal face. (g) Higher resolution atomic scale image for *C. pelagicus* (drift: 0.3 nm/s, scaling: 0.98) and (h) *O. fragilis* (drift: 0.2 nm/s, scaling: 1.03).

tip. Figure 2c is a higher resolution image of some distal shield elements. Each element is slightly tipped and rotated with respect to the last and overlaps like tiles on a roof, so the circumference of the shield is formed from the edges of individual crystals. This view suggests that the element edges might be defined by the edges of the rhomb. The orientation of a 2-dimensional rhombic face would define the a-axis direction but the direction of the c-axis, responsible for determining which edges of the 3-dimensional rhombohedron slope away at obtuse angles from the face shown, is still undefined.

High-resolution images, such as those shown in Figures 2e and 2g, which were taken from elements with circumference edges roughly parallel to the bottom of the page, show the direction of atomic rows along the a-axis (dotted line). The atomic patterns define the size of the surface unit cell (outlined) and they also show row-pairing. The unit-cell geometry matches that expected for the $\{10\bar{1}4\}$ calcite face (Stipp et al. 1994), proving that *C. pelagicus* grows elements directly with the rhombic crystal form. The row-pairing allows determination of the c-axis. On the rhomb shown in Figure 2e, the c-axis emerges from the corner formed by the intersection of the two obtuse edges (marked with an open circle), in a vector at roughly 11 o'clock, perpendicular to the a-axis, at an angle of 51° from the paper. Thus, the rhombohedral elements are oriented so that the shield circumference edge slopes away with an acute angle, and the radial sides, hidden by the next overlapping elements, are also acute edges (marked < on Figs. 2c and 2e). Exposed radial edges slope away with an obtuse angle. Figure 3a shows the orientation of a *C. pelagicus* distal element within the calcite rhomb; each element of the shield has the same orientation.

The other species, *Oolithothus fragilis*, produces thin, delicate shields. Figure 2b shows that only 20 or so wedge-shaped elements are held together by zigzag sutures. Cross-sections from several higher resolution images (not shown) reveal that the outer one-third to one-half of each element is planar whereas the inner shield (such as on the lower right side of Fig. 2d) is a close succession of steps and terraces producing a concave central area.

Figures 2f and 2h show atomic patterns for elements with their circumference edges in the direction of the left side and bottom, respectively. The unit cell matches that expected for the rhombic face, but in the case of *O. fragilis*, the atomic rows are oriented to lie roughly parallel to the coccolith circumference. From row-pairing, the orientation of the c-axis is defined to emerge (from the intersection of the obtuse sides, marked with open circle on Fig. 2f) in a vector at 2 o'clock, pointing 51° from the plane of the paper. Thus, the crystallographic orientation allows the acute rhombohedron edges to form the circumference of the coccolith so that a gentle zigzag makes a thin and curving outer edge and stable, obtuse steps link terraces producing a slope down to the central hollow. The acute corners of the rhomb cleverly interlink at the radial edges of the elements, creating the complex sutures that zipper together the adjacent, almost coplanar elements. Figure 3b shows the relationship of the *O. fragilis* distal shield element to the calcite cleavage rhomb.

DISCUSSION

The biologically produced calcite studied here shows exactly the same atomic-scale features as freshly cleaved, inorganic crystals, making it possible to define crystal orientation. For the two species, the difference in crystallographic orientation corresponds to differences in morphology of the elements, and hence to the shape of the coccoliths and to the coccospheres that they produce. They demonstrate how the thermodynamic drive toward the most stable calcite crystal form, i.e., the rhomb, can be exploited in very different ways. Below, we discuss how coccolith architecture, which is defined by crystallographic orientation, may adapt each species to its ecological niche, through links between morphology and function.

Although coccosphere function is enigmatic, it has been associated with protection, either from predation or by providing a chemical buffer zone, and with light or buoyancy control (Young 1994; Sikes and Wilbur 1982; Baumann et al. 1978; Gartner and Bukry 1969; Braarud et al. 1952). There is also evidence that CaCO_3 production may benefit the cell chemically (Brownlee et al. 1994; McConnaughey and Whelan 1997). Because the producers of coccoliths are photosynthetic marine plankton, they cannot afford to ignore the influence of the coccosphere on their two keys to life—namely, nutrients and light. The density of algae and seawater are similar but

coccosphere production aids sinking. If nutrient uptake is limited by diffusion of nutrients to cells, sinking enhances nutrient supply, and calculations have shown that this effect is significant for rapidly reproducing species in nutrient-limiting conditions (Young 1994; Gavis 1976). However, species that cannot propel themselves must carefully balance the need for sinking into zones of higher nutrients with buoyancy for remaining within the photic zone. Finally, light passage into the cell is determined by calcite crystal thickness as well as orientation, which modifies reflectivity, refraction, and transmittance. Thus, successful architecture must compromise among buoyancy, optics, and possible protection.

Coccolithus pelagicus, which produces thick, robust coccoliths, rapidly sinks through nutrient-enriched waters. An easy way to build heavy coccoliths is to imbricate several rhombic elements. The thickness of the heavy plate and the many internal grain boundaries, where the atomic lattice is mismatched, both decrease light transmittance. Light loss by reflection is maximized because the element surfaces are smooth and the c-axis is near vertical, so the light vibrates in the plane of maximum atomic density. However, because of the orientation of the c-axis and extreme light refraction by calcite, the light that passes through the $\{10\bar{1}4\}$ surface into the coccosphere is bent toward the center of the cell. *C. pelagicus* is one of the dominant species in high latitudes and blooms in the up-welling of nutrient-rich waters, rapidly exploiting suddenly favorable conditions (Baumann et al. 2000; Cachao and Moita 2000; Wells and Okada 1997; Okada and McIntyre 1979). A heavy coccosphere promotes sinking, increasing nutrient accessibility, whereas turbulence ensures its return to the photic zone. There is no need to use extra energy controlling the growth of coccospheres; coccoliths adopting simple rhombohedral faces aid sinking for nutrient accessibility and light collection is sufficient because of a high photic zone habitat.

In contrast, the light and thin architecture of *Oolithotus fragilis* avoids the need for element overlap by interlocking rhomb corners along zigzag sutures. The crystallographic orientation of the distal shield is such that the c-axis is tilted 20 to 35° from normal to the shield (Fig. 3b), a deviation from typical V/R coccolith structure. The net optical result is: reduced reflection because of both crystal orientation and rougher surfaces; increased transmittance because of fewer internal grain boundaries and very thin shields; but decreased refraction. *O. fragilis* builds coccospheres that are much larger than the cell itself (Fig. 1d), meaning that focusing light is of little advantage, but the distribution of the mass of the sphere over a larger surface area decreases density, increasing buoyancy and possibly also contributing a favorable local environment. *O. fragilis*, which lives deep in the photic zone of subtropical waters (Okada and McIntyre 1979; Okada and Honjo 1973), does not bloom, so has no need of rapid exploitation of nutrient supplies. Instead, crystal orientation is adapted for production of thin but strong shields optimized for low light where nutrients are not limiting. Terminal sinking is minimized by coccospheres that approach the density of seawater.

The orientation of the calcite crystals, which make the coccoliths of these two species, determines the properties of the coccospheres of the algae. We suggest that the ability of

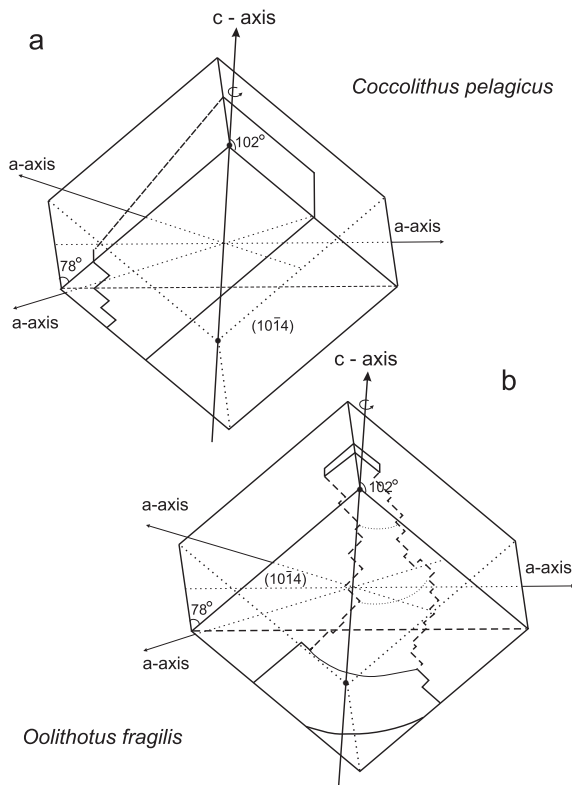


FIGURE 3. Relation of a distal shield element to the calcite cleavage rhomb. Bold dashed line shows the direction of atomic rows, black dots indicate points of entry and exit for the c-axis. (a) *C. pelagicus*, (b) *O. fragilis*.

the species to apply the mineral motif in very different ways is key to their adaptation to their environment. Clearly, millions of years of natural selection have perfected the tailoring of coccolith biocrystals so that the mineral structure of the material is used to the greatest advantage.

ACKNOWLEDGMENTS

We thank Birgit Damgaard, Tonci Balic-Zunic, Knud Dideriksen, Rune Kristensen, Dirk Bosbach, Markus Geisen, Blair Steel, and Ian Probert. Funding to set up the NanoGeoScience lab was provided by the Danish Research Council. Steve Higgins and Mary Marsh are thanked for constructive and thoughtful reviews.

REFERENCES CITED

- Baumann, K.H., Young, J.R., Cachao, M., and Ziveri, P. (2000) Biometric study of *Coccolithus pelagicus* and its palaeoenvironmental utility. *Journal of Nanoplankton Research*, 22, 82.
- Baumann, F.G., Isenberg, H.D., and Gennaro, J. (1978) The inverse relationship between nutrient nitrogen concentrations and coccolith calcification in cultures of the coccolithophorid *Hymenomonas* sp. *Journal of Protozoology*, 25, 253–256.
- Binnig, G. (1992) Force microscopy. *Ultramicroscopy*, 42–44, 7–15.
- Braarud, T., Gaarder, K.R., Markali, J., and Nordli, E. (1952) Coccolithophorids studied in the electron microscope—observations on *Coccolithus huxleyi* and *Syracosphaera carterae*. *Nytt Magasin for Botanik*, 1, 129–134.
- Brownlee, C., Nimer, N., Dong, L.F., and Merret, M.J. (1994) Cellular regulation during calcification in *Emiliania huxleyi*. In J. C. Green and B.S.C. Leadbeater, Eds., *The haptophyte algae*. Systematics Association Special Volume no. 51, 133–148.
- Cachao, M. and Moita, M.T. (2000) *Coccolithus pelagicus*, a productivity proxy related to moderate fronts of Western Iberia. *Marine Micropalaeontology*, 39, 131–155.
- Gartner, S. and Bukry, D. (1969) Tertiary holococcoliths. *Journal of Palaeontology*, 43, 139–142.
- Gavis, J. (1976) Munk and Riley revisited: Nutrient diffusion transport and rates of phytoplankton growth. *Journal of Marine Research*, 34, 161–179.
- Henriksen, K. and Stipp, S.L.S. (2002) Image distortion in scanning probe microscopy. *American Mineralogist*, 87, 5–17.
- Henriksen, K., Young, J.R., Bown, P.R., and Stipp, S.L.S. (2004) Coccolith biomineralization investigated with atomic force microscopy. *Palaentology*, 46, in press.
- McConnaughey, T.A. and Whelan, J.F. (1997) Calcification generates protons for nutrient and bicarbonate uptake. *Earth Science Reviews*, 42, 95–117.
- Ohnesorge, F. and Binnig, G. (1993) True atomic resolution by atomic force microscopy through repulsive and attractive forces. *Science*, 260, 1451–1456.
- Okada, H. and Honjo, S. (1973) Distribution of coccolithophorids in Pacific. *Deep-Sea Research*, 20, 355–374.
- Okada, H. and McIntyre, A. (1979) Seasonal distribution of modern coccolithophores in the western North Atlantic Ocean. *Marine Biology*, 54, 319–328.
- Sikes, C.S. and Wilbur, K.M. (1982) Functions of coccolith formation. *Limnology and Oceanography*, 27, 18–26.
- Sokolov, I.Yu., Henderson, G.S., and Wicks, F.J. (1999) Theoretical and experimental evidence for “true” atomic resolution under non-vacuum conditions. *Journal of Applied Physics*, 86, 5537–5540.
- Stipp, S.L.S. (1999) Toward a conceptual model of the calcite surface: Hydration, hydrolysis and surface potential. *Geochemica et Cosmochemica Acta*, 63, 3121–3131.
- Stipp, S.L. and Hochella Jr., M.F. (1991) Structure and bonding environments at the calcite surface as observed with X-ray photoelectron spectroscopy (XPS) and low energy electron diffraction (LEED). *Geochemica et Cosmochemica Acta*, 55, 1723–1736.
- Stipp, S.L.S., Eggelston, C.M., and Nielsen, B.S. (1994) Calcite surface structure observed at microtopographic and molecular scales with atomic force microscopy (AFM). *Geochemica et Cosmochemica Acta*, 58, 3023–3033.
- Wells, P. and Okada, H. (1997) Response of nanoplankton to major changes in sea-surface temperature and movements of hydrological fronts over site DSDP 594 (south Chatham Rise, southeastern New Zealand), during the last 130 kyr. *Marine Micropalaeontology*, 32, 341–363.
- Young, J.R. (1994) Coccolith function. In W. G. Siesser and A. Winther, Eds., *Coccolithophores*, p 63–82. Cambridge University Press, U.K.
- Young, J.R., Didymus, J.M., Bown, P.R., Prins, B., and Mann, S. (1992) Crystal assembly and phylogenetic evolution in heterococcoliths. *Nature*, 356, 616–618.
- Young, J.R., Davis, S.A., Bown, P.R., and Mann, S. (1999) Coccolith ultrastructure and biomineralisation. *Journal of Structural Biology*, 126, 195–215.

MANUSCRIPT RECEIVED MARCH 18, 2003

MANUSCRIPT ACCEPTED MAY 27, 2003

MANUSCRIPT HANDLED BY ROBERT DYMEK